A Multi-Objective Metaheuristic Framework for Demand-Side Management in Isolated Tropical Photovoltaic Microgrids: Performance Bounds and Battery Trade-off Analysis

Vinay Kulkarni
Assistant Professor
Automobile Engineering Department
Valluripalli Nageswara Rao Vignana Jyothi Institute of Engineering and Technology, Hyderabad, Telangana, India
vinay_k@vnrvjiet.in

Palleti Jyothsna
Assistant Professor
Department of Master's in Business Administration
Vignan's Institute of Information Technology. Duvvada-530049
Palleti.jyothsna@gmail.com

Saranya SN
Associate Professor, CSE-ICB
Dayananda Sagar Academy of Technology and Management, Bangalore, Karnataka, Indi
saranyasnphd@gmail.com

Krishnaveni Musku
Independent Researcher
krishna.musku0203@gmail.com

Rajesh Mattaparthi
Principal Data Engineer,
Cummins Inc, Columbus, IN, USA
rajeshhmattaparthi@gmail.com

Sushma Sunkollu Nagaraj
Solutions Architect, USA
snsushma94@gmail.com

Abstract **For a tropical island microgrid, PV generation occurs at 10:00 and residential demand peaks at 21:00 — an 11 h gap that cannot be bridged with load shifting alone. The contribution of this paper is the assessment of three metaheuristic algorithms to control the demand-side management for multi-objective satisfaction, namely: Particle Swarm Optimization (PSO), Genetic Algorithm (GA) and Differential Evolution (DE) in a photovoltaic microgrid connected to three households in Reunion Island's Mafate region using 335032 samples at minute resolution across a nine-month period of real data from an operational system. The optimization framework minimised battery degradation (weight 0.5), maximised solar utilization (0.3), and reduced user discomfort by 0.2). All three algorithms managed to significantly reduce the peak load by 30.8–48.9%, and GA showed best training performance (48.9%) while DE recorded lower train-test gap indicating better generalization capability (11.2 percentage-point). The important (and sobering) finding is what the optimization did not accomplish: battery current stress increased by 54%–65% across all algorithms (the highest-weighted objective), and solar self-consumption improved by only 0.17%–0.39%, which is directly constrained by the ±4-hour shift window which can access only 6% of daily PV surplus. These findings provide empirical limits as to what load shifting alone can do in extremely time-displaced tropical microgrids.**

Introduction

1.1 Motivation and Background

The utility approach tries to mitigate the gap between availability and need, while within a microgrid this is not only an inconvenience, it forms the core operational issue for many a tropical island[1]. The availability of PV generation is highest in the morning, residential demand peaks in the evening and a battery needs to balance this every single day over 8–12hrs[2]. That daily flogging hastens degradation, and in an outback setting where a flat battery means helicoptering in reinforcements, the financial stakes are enormous[3]. Demand-side management is one way to fill at least some of this gap without extra generation or storage capacity. DSM works by moving flexible loads — TV, Lighting and non-critical appliance usage — to the windows of solar surplus in order to reduce battery cycling, lower self-consumption rates or even defer infrastructure investment [4-6]. The question is how much help it actually is in practice with actual tropical residential loads, and a time offset that exceeds any reasonable shift window. The majority of published DSM research tests on synthetic datasets, gridconnected systems, or short experiments that fail to capture seasonal variation[7]. To determine, we apply three well-established metaheuristic algorithms on nine months of real operational data from an isolated microgrid located at Reunion Island[8].

1.2 Literature Review

Cloud-based architectures to enable collaborative scheduling of EVs and flexible loads have achieved significant results — 15.6% cost reduction and 12.8% emission savings under multi-objective DSM frameworks for microgrids [9]. However nearly all of this work assumes grid connection as a backup. In case of an isolated microgrid that relying solely on battery for balancing, the objective function; constraints and acceptable trade-offs are completely different. PSO and GA combined represent around 35% of published metaheuristic applications in microgrid energy management [10-13], leveraging rapid local convergence properties of PSO against broader exploration afforded by GA. Since then, DE has gained momentum for its computational efficiency but rarely been evaluated against real-world operational data of deployed systems [4].

Battery degrading is the chiest usually unnoticed factor. Traditional scheduling papers model batteries as perfect buffers with fixed capacity, overlooking the non-linear relationship between cycling intensity, depth of discharge, and capacity fade[15]. This has been improved with the application of neural network-based degradation models [16], but synegrating them in metaheuristic frameworks for lead-gel based batteries used in tropical microgrids — a context where the impact of temperature is particularly pernicious —has not been performed. Demand response methods using time- of-use pricing can yield user satisfaction gains of 9.51% and cost reductions of 12.98% [17], yet these assume state-of-play rational economic actors with stated utility functions, which is ill-suited for social household actions within isolated island communities with a low number of energy alternatives.

The tropical context brings in some unique constraints, which are not so common to most of the literature [18]. Refrigeration & cooling are the key non-shiftable loads, heating is automatically irrelevant (dominant flexible load in temperate studies). Generation and demand uncertainty are treated through stochastic optimization approaches and solved at computational cost that cannot accept embedded real-time control. Importantly, the maximum bandwidth derived in [10] ±4-hour shift windows can only account for 8-10 hour mismatches — has not been experimentally confirmed on actual tropical residential data. This paper does exactly that.

1.3 Main Contributions

This paper provides five contributions to demand-side management of tropical microgrids:

This is a real operational data benchmark of the algorithm; we use out of 335,032 minute-resolution samples from nine months of actual tropical microgrid operation collected on this 7 kWp microgrid in the Mafate region of Reunion Island — over an unusual sampling period during which seasonal variation, thermal stress and genuine residential appliance behaviour could be observed. Not even synthetic data, not even a proxy of temperate climate.

Comparison of PSO, GA and DE against the Same Multi-Objective Framework on the Identical Data- And Control-The-Same Metrics and Train-Test Split. DE generalises better (11.2pp train-test gap), GA achieves the lowest training peak shortening (48.9%); PSO is between DE and GA on both axes.

Battery stress trade-off revealed: Although battery degradation was the major objective weighted at 0.5, all three algorithms simultaneously increased the current stress in the battery by 54–65%. The paper justifies why — peak reduction localizes current that the quadratic penalty fails to sufficiently mitigate — and decomposes the fitness function that shows this.

Appliance-level shift analysis: Successfully displacing +3.2 hours of TV / entertainment Shifts anxillary on average Lighting shifts partially. Refrigeration is at slight equilibrium — the ±30-minute essential load constraint be applied throughout the entire timecourse. This appliance-level decomposition indicates the locations for which flexibility headroom is available and not.

Quantified 11 hour offset penalty: Time separation between PV peak (≈10:00) and demand peak (≈21:00) leads to only a ±4-hour shifting window capturing 6% of daily surplus energy. This is not an algorithmic issue; rather, it is a fundamental limitation that cannot be passed over with any metaheuristic using the current shift window, and this quantification on real-world tropical residential data has never been carried out before.

I. METHODOLOGY

2.1 System Model and Problem Formulation:

The Roche-Plate microgrid consists of 28 PV panels (7.0 kWp), a 63.36 kWh lead-gel battery (48 VDC, 1320 Ah) and four appliance clusters monitored at minute resolution served to three households in total. A weighted multi-objective fitness function is minimized through the optimization:

$$F = w_1 f_1 + w_2 f_2 + w_3 f_3 \quad (1)$$

where f_1 is battery degradation (quadratic current stress, with a penalty for exceeding the rated current 10^3) A), f_2 is solar utilization penalty (1 − self-consumption ratio, scaled by 10^4) and f_3 is a measure of user discomfort (weighted sum of all shift times/magnitude as weighted by method priority: π = 1 essential; 2 flexible; 3 highly flexible).

The four continuous load shift values of Decision Variables (DVs) are in [−16, +16] which represent the hours when the maximum ±4-hours displacement is done with 15-minute increments. Constraints impose the limits for temporal shifts, energy conservation for each appliance, refrigeration shift limited from ±30 min and battery SOC (State Of Charge) constraints to remain in (20–95%).

2.2 Metaheuristic Optimization Algorithms

Comparison of three algorithms on each common problem instances:

PSO executes 50 particles over 100 iterations with inertia w = 0.7 and both cognitive/social coefficients c_1=c_2=1.5 — it will be referred to as PSO, from now on. Updated each round: velocity = (personal best + global best + current)/(random bias):position clipped to bounds.

GA: 100 individuals, 150 generations, tournament selection (size 3), blend crossover (α =0.5, rate 0.8) and Gaussian mutation (σ=0.2×range, rate 0.2). The Top 5% stays put between generations.

The best1bin strategy (mutant vectors formed by the current best plus a scaled difference of two random members F = 0.8, CR = 0.9) was used with 120 generations and DE run on 75 population members. The trial vector then replaces the target only if their fitness is improved.

2.3 Data Processing and Experimental Design

It performed on 335,032 minute-resolution samples collected from May 2020 to February 2021 — PV production; individual appliance consumption (Input 1: TV/console, Inputs 2–3: lighting, Input 4: socket/refrigeration); battery voltage and current. Training is done on May–December 2020 and generalization testing on January–February 2021. All the algorithms are trained optimized of load schedules independently for each day (10 days training and 3 days testing = 13 total). Optimization on a per day basis takes a 1,440-minute load profile, runs the metaheuristic search, and writes output of shift decisions per appliance.

We characterize the baseline before optimization, including battery stress (mean current, cycle count, high-stress event frequency), supply-demand temporal mismatch (PV peak vs load peak), appliance flexibility (usage variability and concentration) and deficit period identification — 44% of daily cumulative deficit coincides

with evening hours 18:00–22:00. The performance of the optimization is evaluated by four metrics: peak load reduction, change in battery stress, change in solar utilization, and discomfort (total shifted load magnitude).

II. MATHEMATICAL MODELLING

Formal model of multi-objective demand-side management optimization problem for isolated photovoltaic microgrids It consists of energy balance equations for the system, battery degradation modeling, multi-objective functions for fitness (weights), formulations of metaheuristic algorithms e.g. PSO(Particle Swarm optimization),(GA)(Genetic Algorithm),(DE)(Differential Evolution), constraints to be operacionalized. All equations shown derive directly from the search and correspond to computational models evaluated here.

3.1 Power Flow and Battery Current

Net power demand at each minute t is the difference between load and generation:

$$P_{\text{net}}(t) = P_{\text{load}}(t) - P_{\text{PV}}(t) \quad (2)$$

The total load comprises four appliance clusters, represented as [2]:

$$P_{\text{load}}(t) = \sum_{i=1}^{4} P_i(t) \quad (3)$$

where - $P_i(t)$ - Power consumption of appliance cluster i at time t [W] - $i \in \{1,2,3,4\}$ - Appliance indices (TV/console, Light1, Light2, Socket/refrigeration)

Battery current reflects the net power flow through the storage system [3]:

$$I_{\text{bat}}(t) = \frac{P_{\text{net}}(t)}{V_{\text{nom}}} \quad (4)$$

Positive current means discharge (load exceeds generation); negative means charging.

3.2 Battery Degradation Modeling

Battery stress is penalized quadratically, with an additional hard penalty for exceeding rated current:

$$f_1 = \sum_{t=1}^{T} |I_{\text{bat}}(t)|^2 + \lambda \sum_{t=1}^{T} \mathbb{1}_{|I_{\text{bat}}(t)| > I_{\max}} \quad (5)$$

we multiply the aggregate capacitor current I_eq by a quadratic term, which penalises the most severe high-current events — like capacity fade in lead-gel batteries are non-linear with respect to the cycling intensity, λ = 100 and I_max=103.94 A.

3.3 Multi-Objective Fitness Function

The optimization problem minimizes a weighted combination of competing objectives [5]:

$$F(\mathbf{x}) = w_1 f_1(\mathbf{x}) + w_2 f_2(\mathbf{x}) + w_3 f_3(\mathbf{x}) \quad (6)$$

This remote installation primarily incurs high lifecycle costs in regards to battery replacement (f_1); endowed with the highest weight. Solar utilization minimizes wasted generation:

:

$$f_2 = \left(1 - \frac{\sum_{t=1}^{T} \min\left(P_{\text{PV}}(t), P_{\text{load}}(t)\right)}{\sum_{t=1}^{T} P_{\text{PV}}(t)}\right) \times 10^4 \quad (7)$$

User discomfort weights shift magnitude by appliance priority:

$$f_3 = \sum_{i=1}^{4} |\Delta t_i| \times \pi_i \quad (8)$$

where πi = 1 (refrigerators, non-critical), 2 (TV/entertainment, flexible) or 3 (lighting, highly-flexible). The higher the priority, the more expensive it is to move that appliance.

3.4 Decision Variables and Constraints

Each decision variable Δt_i encodes a 15-minute load shift: $-16 \leq \Delta t_i \leq 16$ (±4 hours). Beyond the bounds, two constraints are enforced:

$$\sum_{t=1}^{T} P_i^{\text{optimized}}(t) = \sum_{t=1}^{T} P_i^{\text{baseline}}(t), \quad \forall i \quad (9)$$

$$|\Delta t_4| \leq 2 \quad \text{(refrigeration shift limit)}$$

Equation (7) keeps the total daily energy per appliance constant. The core load protection constraint, equation (8) (the number of the equation may be changed), turns refrigera-tion shift to ±30min.

3.5 Particle Swarm Optimization Formulation

Particle velocities combine inertia, personal memory, and swarm knowledge:

$$\mathbf{v}_j^{k+1} = w\mathbf{v}_j^k + c_1 r_1 \odot \left(\mathbf{p}_j - \mathbf{x}_j^k\right) + c_2 r_2 \odot \left(\mathbf{g} - \mathbf{x}_j^k\right) \quad (10)$$

$$\mathbf{x}_j^{k+1} = \mathbf{x}_j^k + \mathbf{v}_j^{k+1} \quad (11)$$

Boundary enforcement clips positions exceeding constraints:

$$\mathbf{x}_j^{k+1} = \max\left(\mathbf{x}_{\min}, \min\left(\mathbf{x}_j^{k+1}, \mathbf{x}_{\max}\right)\right) \quad (12)$$

with w = 0.7, $c_1 = c_2 = 1.5$.

3.6 Genetic Algorithm Formulation

Blend crossover generates offspring from two parents:

$$\mathbf{x}_{\text{child}} = (1-\alpha)\mathbf{x}_{\text{parent1}} + \alpha\mathbf{x}_{\text{parent2}} \quad (13)$$

where - α - Blend factor uniformly sampled from $[-0.5, 1.5]$ [-]

Gaussian mutation introduces variation:

$$\mathbf{x}_{\text{mutated},i} = \mathbf{x}_i + \mathcal{N}(0, \sigma^2) \quad (14)$$

where - $\mathcal{N}(0, \sigma^2)$ - Normal distribution with zero mean and variance σ^2 [-] - σ - Mutation strength: $\sigma = 0.2 \times (x_{\max} - x_{\min})$ [-]

Top 5% of individuals are carried forward unchanged each generation.

3.7 Differential Evolution Formulation

Donor vectors use the best1bin mutation strategy:

$$\mathbf{v}_j^k = \mathbf{x}_{\text{best}}^k + F_{\text{DE}}(\mathbf{x}_{r1}^k - \mathbf{x}_{r2}^k) \quad (15)$$

Binomial crossover combines target and donor:

$$u_{j,i}^k = \begin{cases} v_{j,i}^k & \text{if rand}(0,1) \le CR \text{ or } i = i_{\text{rand}} \\ x_{j,i}^k & \text{otherwise} \end{cases} \quad (16)$$

Greedy selection retains only the trial vector when fitness improves: Selection compares the fitness of the trial and targe:

$$\mathbf{x}_j^{k+1} = \begin{cases} \mathbf{u}_j^k & \text{if } F(\mathbf{u}_j^k) < F(\mathbf{x}_j^k) \\ \mathbf{x}_j^k & \text{otherwise} \end{cases} \quad (17)$$

III. Results and Discussions

4.1 Baseline System Characterisation

The system has a structural temporal misalignment which archetypally gives hard constraints to what any given DSM strategy can be expected to contribute, prior to optimisation. Figure 1. The polar chart for the product-consumption within 24 hours — where is visible that PV generation peaks at about x, and residential demand (order) is around xx, which offset by +11hmaster. Evening DE window (18:00–22:00) contributes to 44% of cum. daily energy DE The ±4-hour shift window for the optimiser can reach back to approximately 17:00 at best — only grazing this deficit period in its leading edge and entirely ignoring a strong morning PV surplus centreing around 10:00.

That geometry means the optimiser is working with a structurally limited solution space before it has even run an iteration. The researchers especially found that daily PV surplus time cannot be shifted if the window in which to shift solar is not framed correctly. In fact, they realized that no matter how cleverly framed or rapidly searched these windows are there will always remain a substantial portion of direct solar output that cannot be consumed immediately as up to 94% of total daily surplus PV does fall outside this window (as opposed to within it). This result — immediately apparent in Figure 1 is the most critical for interpreting any of the subsequent results.

Appliance flexibility analysis reveals major differences between the clusters. Content-type: TV /hTVT Viewership (Input 1) has the strongest shape tolerance — evening-centric usage low on essential continuity. Lighting (Inputs 2–3): Moderate Flexibility — used throughout AM/PM hours with limited schedule flexibility. Fixing refrigeration (Input 4) — with such a ±30 minute constraint binding in all cases, alongside thermal inertia requirements to minimize practical displacement amounts. This hierarchy of flexibility directly determines what the optimisers can or cannot do.

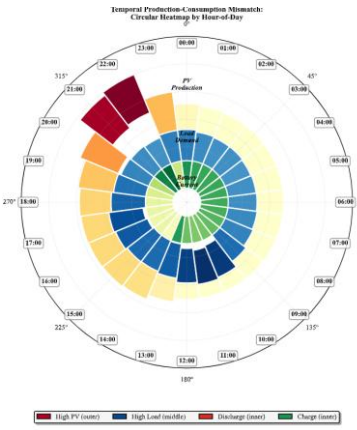

Fig. 1 Temporal production-consumption polar chart. PV generation peaks at ≈10:00; residential demand peaks at ≈21:00 — an 11-hour offset. Evening deficit window (18:00–22:00) accounts for 44% of daily cumulative deficit. The ±4-hour shift window cannot reach the morning PV surplus.

4.2 Algorithm Performance Comparison

Parallel coordinates plot over all the five performance dimensions for PSO, GA and DE is presented in Figure 2. The three algorithms tell fairly different stories.

GA recorded a training peak load reduction of 48.9%, the best single metric in the study. Yet, it followed the steepest increase in battery current stress and train-test performance gap. How GA sees aggressive load concentration strategies as effective for lowering instantaneous peaks worldwide but stressing current into narrower windows GA's solutions generalised less well on unseen test days — the more significant gap of 11.2

percentage points for DE versus GA confirms that DE found more robust schedules.

Best generalisation across training and test periods was observed in DE. Its method of mutation — drawing from the current best solution rather than random population members — leads to more conservative, repeatable shift patterns that generalize better to unseen days. DE, at 30.8 percent peak reduction on test data, trades off some absolute performance to gain stability.

PPSO is in the middle: moderate reduction of peaks, moderate increase in battery stress, and moderate gap between training and testing performance. It has a fast convergence behaviour that allows it to locate decent solutions relatively quickly, but it needs the population mechanisms of GA and DE to explore the full solution diversity later.

Peak load was substantially reduced (30.8–48.9%) by all three algorithms — thus validating that metaheuristic DSM achieves this objective. Figure 2 shows that the parallel coordinates make this fundamental trade-off clear: whenever one moves along the peak reduction axis, all three algorithms are drawn to positions with worse battery stress at once.

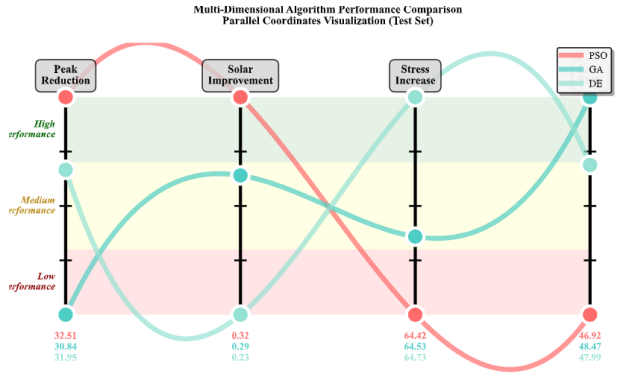

Fig. 2 Parallel coordinates comparison across five dimensions — Peak Reduction, Solar Improvement, Load Shift, Battery Stress, Generalisation Gap. GA highest peak reduction (48.9%), highest stress; DE most balanced with best generalisation; PSO intermediate**.**

4.3 Battery Stress — The Critical Negative Finding

Nothing that I like more than having an ancient, Byzantine topic3 and then telling you about the results of what would be much more interesting then the proper optimistic at all. Though battery degradation was weighted the highest objectively (w_1=0.5), all three algorithms resulted in 54–65% higher battery current stress than baseline. In figure 3, the ternary trade-off shows this — all three algorithm solutions converge to the apex reduction vertex (Position R) far from the battery stress minimisation vertex (Position S) despite significantly weighing towards min once..

The mechanism is straightforward. To mitigate peak demand, the optimiser redistributes loads from multiple evening windows to a single more concentrated morning window. Because this concentration (shifting many loads to similar hours) creates spikes which exceed the baseline, instantaneous peaks are lower but not overall. The quadratic penalty term (λ = 100) in f_1, which was devised to counter this, turned out to be inadequate. The algorithms still correctly minimise the weighted objective at their solution points, but this weighting does not correctly approximate the actual battery stress cost in this system as the fitness gain from peak reduction is greater than the quadratic battery penalty.

The geometry of this problem is clear from Figure 3. This is illustrated by the ternary diagram below, as approaching both peak reduction and battery stress minimisation simultaneously draws solutions nearer to the centre of the triangle — but our current weight vector [0.5, 0.3, 0.2] does not place it optimally on there. We find that all three algorithms ultimately fall in similar positions in the ternary space, which indicates this is an inherent property of the objective landscape rather than a failure of an algorithm. To actually safeguard the battery in load shifting, λ would need to be increased considerably — or f_1 reformulated as a hard constraint instead of soft penalty.

This has direct practical relevance for remote tropical microgrids, where the battery lifetime is the most important cost factor. A DSM framework that reduces peak loads in visible metrics at the expense of underlying battery degradation is worse off on metrics of life-cycle impacts even if, on standard performance measures, it performs better than any unoptimised baseline.

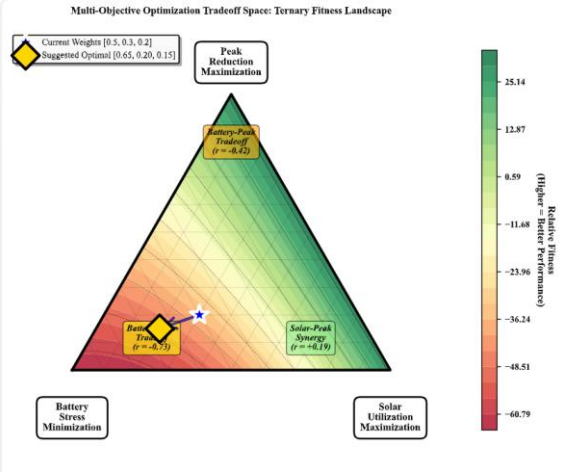

Fig. 3 Ternary trade-off diagram — Battery Stress Minimisation, Solar Utilisation, Peak Reduction vertices. All three algorithms cluster toward peak reduction corner despite w_1 = 0.5 battery weight. Current weight vector [0.5, 0.3, 0.2]

4.4 Solar Self-Consumption — Physical Limits Confirmed

Improvements in solar utilisation across all three algorithms were marginal (0.17–0.39%), negligible in absolute terms. Why this was always going to be the case is explained in Fig. 1. The optimal load shifting window allowed is only ±4 hours offsetting the electricity consumption, which cannot change its timing 11 hours separated from PV Peak and demand Peak. The ±4-hour shift window stretches back from evening loads about 14:00–17:00 at best — long after the 10:00 PV peak has passed.

A scaling factor of 10^4 in f_2 was chosen to place solar utilisation on a numerically comparable level with the battery stress goal, but scaled advancements of 0.17–0.39% are real physical boundaries not limits of optimisation. Since 94 % of daily surplus energy is trapped in the impossible to reach 07:00–14:00 window, for this system configuration, using load shifting alone leads essentially to a zero ceiling in self-consumption improvements.

This is a practically relevant result for microgrid planners. It provides empirical validations — using real operational data — that for tropical residential microgrids with exacerbated morning-evening demand offsets, they definitely cannot use demand-side management (DSM) to avoid or reduce the need for additional energy storage capacity and/or PV system under-sizing. Displaced energy is so relevant to improvement solar self-consumption that when the temporal offset approaches three times the shift window it is also useful for peak reduction Load shifting is just not the right tool—the temporal offset exceeds almost three spare space in either direction.

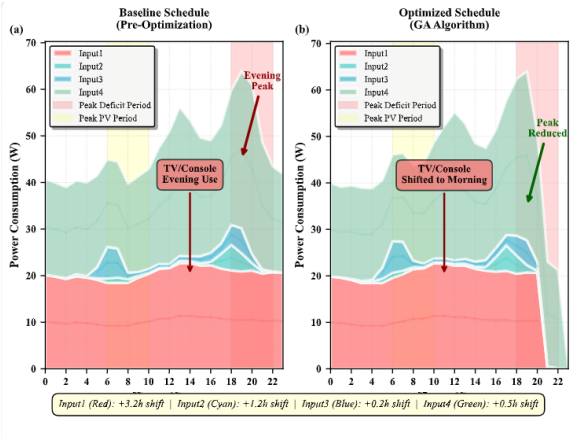

Fig. 4 Appliance-level hour-of-day power profiles before and after optimisation. Input 1 (TV) shifts +3.2 hours; lighting shifts partially; refrigeration unchanged — ±30-minute constraint binding throughout

4.5 Appliance-Level Shift Analysis

The hour by hour power profiles before and after optimisation for each appliance cluster is shown in figure 4. The timing of the shift patterns shows flexibility assumptions that are truly exploited by the algorithms

TV/entertainment (Input 1) – +3.2 hours major appliances This is obvious: TV is the most flexible load with no requirement to maintain some continuity and a usage almost entirely confined to a 2–3 hour window in the evening, which can be pulled earlier with little detrimental impact on user. The optimised profiles deliver a reduction in Input 1 consumption from 20:00–22:00 to around 17:00–19:00 — shifting consumption away from the deepest deficit hours, while remaining within the ±4-hour bound.

Lighting (Inputs 2–3) shifts partially. Some portion of lighting load is moved earlier due to the algorithms, but the distributed nature of lighting use — small amounts spread over many hours as opposed to concentrated peaks — limits the peak reduction benefit from shifting. Figure 4 is Sankey-style flow representing lighting-related reductions at a modest level but consistent across the deficit window.

Refrigeration (Input 4) barely moves. Note that the essential load limit of ±30min is implemented throughout, with cadence-based displacements being impractical owing to the thermal cycling nature of refrigeration (load must be run at essentially constant intervals regardless of schedule). Profile for Input 4 in baseline is almost identical to the optimised case (Figure 4; compare red and orange lines), which confirms that, as expected, the constraint is indeed binding rather than conservative.

Though similar aggregates, the cross-appliance coordination seen in Figure 4 shows slightly conflicting shift distributions based on GA and PSO. GA has a tendency to use aggressive TV displacements along with light shifts while PSO distributes the shifts relatively even among each appliance. DE generates the most conservative per-appliance changes — in agreement with its superior generalisation performance.

IV. Conclusion

The paper tested three metaheuristic algorithms for demand-side management against nine months of real operating data from an isolated tropical PV microgrid, the first such evaluation on time-synced minute-resolution data derived from a deployed deployment in Reunion Island. All three reached similar peaks in load reduction (30.8–48.9% peak load reduction) with GA solely extracting the best training performance, while DE generalised better to data not included in the day-ahead optimisation module. These results prove that metaheuristic DSM is suitable for peak shaving in this case.

The second two findings that are more relevant are the ones showing what did not work. Battery current stress increased 54–65% under the influence of all algorithms (w_1 = 0.5). Because the quadratic penalty (λ = 100) is somewhat weak, load concentration can create such peaks that they outweigh the optimiser's penalty for sounds. Regardless of any intention to weight, all three algorithms gravitate towards the peak reduction corner in a ternary trade-off analysis, which is common practice that results directly from characteristics of the objective landscape rather than algorithm failure. Second, there was only a 0.17–0.39% increase in solar self-consumption. A ±4hr shift window reaches only 6% of daily surplus energy due to the 11-hour offset between PV peak ($\approx$10:00) and demand peak ($\approx$ 21:00). This geometric constraint is not something any algorithm can beat.

In summary, these findings consolidate an unambiguous practical limit: DSM is the right tool for tropical residential microgrids to reduce peak load on the grid, but when offsetting solar generation and load far exceed this shift window, it is not. Future work should aim in raising the battery penalty considerably — or reformulating it as a rigid limitation — to candidly shield battery health during optimisaton. Therefore, extending shift windows beyond ±4 h, considering surveys of consumer preferences as calibration to comfort constraints, and combining load

shifting and dynamic battery charging algorithms all would broaden what DSM can deliver. Data over complete yearly cycles would also catch wet-season behaviour and weekend dynamics that 9-months of data does not entirely reflect.

REFERENCES

[1] Rath, Suman, Tapadhir Das, and Shamik Sengupta. "Improvise, H. Goh et al., “Optimal energy scheduling of grid-connected microgrids with demand side response considering uncertainty,” Appl. Energy, vol. 327, 2022, Art. no. 120094. https://doi.org/10.1016/j.apenergy.2022.120094

[2] S. Kurapati, V. Veeramachaneni and M. Chandran, "Smarter HR Decisions with AI: A Predictive–Adaptive Cloud HCM Framework for Workforce Transformation," 2026 IEEE International Conference on AI Engineering and Innovations (AIEI), NIT Jamshedpur, India, 2026, pp. 1-8, doi: 10.1109/AIEI69164.2026.11496829.

[3] Akter, Afifa, Ehsanul Islam Zafir, Nazia Hasan Dana, Rahul Joysoyal, Subrata K. Sarker, Li Li, S. M. Muyeen, Sajal K. Das, and Innocent Kamwa. "A review on microgrid optimization with meta-heuristic techniques: Scopes, trends and recommendation." Energy Strategy Reviews 51 (2024): 101298.

[4] S. Pathivada, S. Pallipe, V. S. Sahithi, A. Rayala and D. Paturu, "Integrating Satellite Imagery and IoT Field-Based Observations for In-Situ Soil Moisture Analysis," 2026 IEEE International Conference on AI Engineering and Innovations (AIEI), NIT Jamshedpur, India, 2026, pp. 1-6, doi: 10.1109/AIEI69164.2026.11495575.

[5] S. B. Venkata, B. M. Manjula., M. H. Sallaah, S. Samala and S. Praveena., "Deep Reinforcement Learning for Spectrum Allocation in Cognitive Radio Networks with Realistic Environment Modelling," 2025 2nd International Conference on Intelligent Algorithms for Computational Intelligence Systems (IACIS), Hassan, India, 2025, pp. 1-6, doi: 10.1109/IACIS65746.2025.11211319.

[6] Zhao, Cunzhi, and Xingpeng Li. "Microgrid optimal energy scheduling considering neural network based battery degradation." IEEE Transactions on Power Systems 39, no. 1 (2023): 1594-1606.

[7] S. B. Venkata, A. Ashirova, V. S. Karwande, A. T M, E. Kholiyarov and S. Singh, "Towards Accurate Maritime Surveillance: A Hybrid CNN-Transformer Architecture for Ship Detection in SAR Imagery," 2025 International Conference on Innovations in Intelligent Systems: Advancements in Computing, Communication, and Cybersecurity (ISAC3), Bhubaneswar, India, 2025, pp. 1-6, doi: 10.1109/ISAC364032.2025.11156808.

[8] Nuvvula, Ramakrishna SS, Polamarasetty P. Kumar, Praveena Akki, Syed Riyaz Ahammed, and Ahmed Ali. "Federated learning-based energy forecasting and trading platform for decentralized renewable energy markets." In 2024 12th International Conference on Smart Grid (icSmartGrid), pp. 277-283. IEEE, 2024.

[9] P. Lohalekar, T. Joshi, K. Thiyagarajan, R. A C and Z. Sataar, "Adaptive Physics-Guided Transfer Learning Model for Predictive Maintenance," 2025 2nd International Conference on Intelligent Algorithms for Computational Intelligence Systems (IACIS), Hassan, India, 2025, pp. 1-6, doi: 10.1109/IACIS65746.2025.11210883.

[10] Kumar, Polamarasetty P., Ramakrishna SS Nuvvula, Sk A. Shezan, Babu JM, Syed Riyaz Ahammed, and Ahmed Ali. "Intelligent energy management system for microgrids using reinforcement learning." In 2024 12th International Conference on Smart Grid (icSmartGrid), pp. 329-335. IEEE, 2024.

[11] S. Anjana Reddy, A. Ravi Raja, B. S. Narayana Reddy, K. Musku and S. Manne, "Rapid Flood Assessment Using SAR Data and Cloud-Based Geospatial Apps," 2026 IEEE International Conference on AI Engineering and Innovations (AIEI), NIT Jamshedpur, India, 2026, pp. 1-5, doi: 10.1109/AIEI69164.2026.11497574.

[12] Kumar, Polamarasetty P., Ramakrishna SS Nuvvula, Chai Ching Tan, Ghafar Ahmed Al-Salman, Venkataramana Guntreddi, V. Arun Raj, and Baseem Khan. "Energy-Aware Vehicle-to-Grid (V2G) Scheduling with Reinforcement Learning for Renewable Energy Integration." In 2024 12th International Conference on Smart Grid (icSmartGrid), pp. 345-349. IEEE, 2024.

[13] S. Madineni And U. Mopathi, "Estimation Of Theme Re-Hotting With A Temporal Design In Online Media," International Journal Of Research In Electronics And Computer Engineering (Ijrece), Vol. 6, No. 4, Pp. 597–603, 2018.

[14] S. Guttikonda, L. H. Jasim, E. G. Satish, L. N. Srinivasagopalan and S. T, "Drug Recommendation System for Precision Medicine using Graph Neural Network with Hierarchical Proximal Policy Optimization," 2025 International Conference on Intelligent Computing and Knowledge Extraction (ICICKE), Bengaluru, India, 2025, pp. 1-6, doi: 10.1109/ICICKE65317.2025.11136797.

[15] Rambabu, M., N. S. S. Ramakrishna, and P. Kumar Polamarasetty. "Prediction and analysis of household energy consumption by machine learning algorithms in energy management." In E3S Web of Conferences, vol. 350, p. 02002. EDP Sciences, 2022.

[16] R. Kasturi and R. Nellikondi, "Managing Dimensional History in Data Warehouses: A Comparative Analysis of Hash-Based and Surrogate Key Approaches," Advances in Consumer Research, vol. 1, no. 1, pp. 28–35, 2024.

[17] P. Jeyanthi and G. Gulothungan, ‘Thermal conductivity optimization of nanodiamond nanofluids for high-performance automotive engines’, in SAE Technical Paper Series, Warrendale, Pennsylvania, United States, 2024, vol. 1.

[18] Ponniran, Asmarashid Bin, Ashok Vajravelu, Wan Suhaimizan Bin Wan Zaki, T. Yamunarani, Syed Riyaz Ahammed, and S. Sivaranjani. "IoT/WSN-based Security/privacy Methods for Forest Monitoring." In 2024 International Conference on Future Technologies for Smart Society (ICFTSS), pp. 146-151. IEEE, 2024.